Observation of the Exotic Isotope ^{13}F Located Four Neutrons beyond the Proton Drip Line

R. J. Charity, T. B. Webb, J. M. Elson, D. E. M. Hoff,* C. D. Pruitt, and L. G. Sobotka
Departments of Chemistry and Physics, Washington University, St. Louis, Missouri 63130, USA

K. W. Brown, G. Cerizza, J. Estee, W. G. Lynch, J. Manfredi,† P. Morfouace, C. Santamaria, S. Sweany, C. Y. Tsang, M. B. Tsang, Y. Zhang, and K. Zhu
National Superconducting Cyclotron Laboratory, Michigan State University, East Lansing, Michigan 48824, USA

S. A. Kuvin, D. McNeel, J. Smith, and A. H. Wuosmaa
Department of Physics, University of Connecticut, Storrs, Connecticut 06269, USA

Z. Chajecki
Department of Physics, Western Michigan University, Kalamazoo, Michigan 49008, USA

(Received 16 November 2020; revised 22 January 2021; accepted 24 February 2021; published 30 March 2021)

A ^{13}F resonance was observed following a charge-exchange reaction between a fast ^{13}O beam and a ^{9}Be target. The resonance was found in the invariant-mass distribution of $3p + ^{10}$C events and probably corresponds to a $5/2^+$ excited state. The ground state was also expected to be populated, but was not resolved from the background. The observed level decays via initial proton emissions to both the ground and first 2^+ state of ^{12}O, which subsequently undergo $2p$ decay. In addition, there may also be a significant proton decay branch to the second 2^+ level in ^{12}O. The wave function associated with the observed level may be collectivized due to coupling to the continuum as is it located just above the threshold for proton decay to the 2^+_2 state of ^{12}O.

DOI: 10.1103/PhysRevLett.126.132501

With the interest in nuclei with large differences in their numbers of protons and neutrons, efforts have been made to extend the chart of nuclides out to the drip lines and beyond. As the widths of low-lying resonances generally increase as one moves further beyond a drip line, the limits to which one can still identify new resonances is determined by our ability to separate wide resonances from the background processes. However, if a relatively narrow resonance is observed far beyond a drip line, it would point to some interesting nuclear structure.

The lightest particle-stable fluorine isotope is ^{17}F. Three lighter isotopes (^{14}F, ^{15}F, and ^{16}F) are known beyond the proton drip line, with ^{14}F having been observed in only one study [1]. Resonance states in all three isotopes have been identified via elastic proton scattering on particle-stable oxygen isotopes [1–6]. In principle, these resonances could also be produced in transfer reactions where a proton is added to the neighboring oxygen isotope. However, with ^{13}O the lightest particle-stable oxygen isotope, proton scattering and transfer reactions cannot be used to find the next lightest fluorine isotope ^{13}F. Alternatively a charge-exchange reaction on ^{13}O would seem a promising approach. Indeed, charge-exchange reactions with a fast ^{17}Ne beam and ^{9}Be target led to the first identification of ^{17}Na [7]. In this Letter, we use a fast ^{13}O beam with a ^{9}Be target to produce and identify a ^{13}F state. Like the ^{17}Na study, the observed resonance is probably not the ground state (g.s.).

Large excursions beyond the proton drip line are expected to be less likely for very light nuclei with only a small Coulomb barrier to constrain the excess protons. The isotope ^{13}F is located four neutrons away from the proton drip line, which represents one of the largest excursions from the proton drip line in light nuclei with only the recent observation of the heavier ^{31}K [8] isotope having the same separation in neutron number. Such remote isotopes will decay by multiple proton emission as there are no proton-bound isotopes located immediately below them in the chart of nuclides. For example, low-lying ^{31}K states were observed to decay by emission of three protons [8]. As the $1p$ and $2p$ daughters of ^{13}F (^{12}O and ^{11}N) are particle unstable, low-lying ^{13}F states should also decay by the emission of three protons. Emitting three protons is the general expectation when crossing the proton drip line using charge-exchange reactions with an even-Z projectile on the drip line. For example, the ^{17}Na resonance produced with the proton drip line ^{17}Ne beam decayed to the $3p + ^{14}$O channel.

An $E/A = 69.5$-MeV secondary beam of ^{13}O was produced from the Coupled Cyclotron Facility at the National Superconduction Cyclotron Laboratory at

Michigan State University from an $E/A = 150$-MeV primary ^{16}O beam. The beam was purified using the A1900 magnetic spectrometer and the radio frequency fragment separator [9], giving an intensity of 10^3 pps with purity of 80%. Forward-emitted charged particles produced in the collisions were detected in the high resolution array (HiRA) [10] located 80-cm downstream of the 1-mm-thick Be target and covered scattering angles from 2.1° to 12.4°. The array contained 14 E–ΔE telescopes, each consisting of a 1.5-mm-thick double-sided Si strip ΔE detector followed by a 4-cm-thick CsI(Tl) E detector. The ΔE detectors are 6.4×6.4 cm in area, with each face divided into 32 strips. Each E detector consisted of four separate CsI(Tl) elements, each spanning a quadrant of the preceding Si detector. Data from this experiment pertaining to the formation of ^{11}O, ^{11}N, ^{12}O, and ^{12}N resonances have already been published in Refs. [11–13], where a discussion of the energy calibrations of the detectors is also given. After the charge-exchange reaction, the resulting ^{9}Li "target" fragment or its decay products, if it was strongly excited, were not detected in the angular and energy acceptance of the array.

The total kinetic energy released in the decay of ^{13}F levels (the decay energy) is denoted by E_T. Experimentally, it is determined from the measured invariant mass of the decay products less the sum of their ground-state masses. The E_T distribution for $3p + {}^{10}$C events detected with the ^{13}O beam is shown in Fig. 1 as the histogram. A peak at $E_T \approx 7$ MeV is resolved above a broad background. The invariant-mass resolution has a strong dependence on the recoil angle of the ^{10}C fragment in the parent ^{13}F center-of-mass frame, with the best resolution occurring for recoils emitted transversely to the beam [14,15]. The plotted spectrum has a $|\cos\theta_H| < 0.5$ gate applied where θ_H is the recoil angle of the ^{10}C fragment in the parent's reference frame with respect to the beam axis. This gate provides a compromise between resolution and statistics.

The solid red curve shows a fit to this spectrum with a single ^{13}F peak and a smooth background (solid blue curve). In the fit, the intrinsic line shape of the peak has been modified to include the effects of the experimental resolution as determined from Monte Carlo simulations of the experiment [14]. The fitted centroid and width of the peak are $E_T = 7.06(9)$ and $\Gamma = 1.01(27)$ MeV, respectively. At this decay energy, the simulated experimental E_T resolution is 525 keV (FWHM). The fitted peak corresponds to a cross section of 60(35) μb determined using a detector efficiency and normalization determined in a similar manner to that described for ^{12}O and ^{12}N cross sections from the same dataset in Ref. [16].

It is possible that the peak is associated with a $3p$ decay of a ^{13}F state leading to the particle-stable first excited state of ^{10}C at $E^* = 3.353$ MeV rather than the ground state as assumed. However, this implies a larger invariant mass, which is unlikely as the expected decay width would probably be larger and the state not resolved.

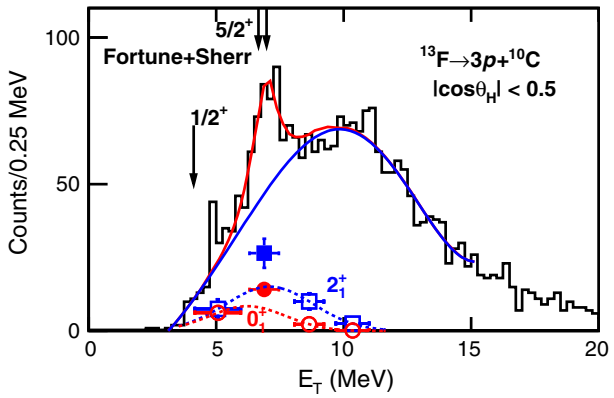

FIG. 1. The histogram displays the spectrum of decay energy for ^{13}F determined from the invariant mass of $3p + {}^{10}$C events. The transverse emission gate $|\cos\theta_H| < 0.5$ was applied. The solid red curve shows a fit to this spectrum with a single ^{13}F peak plus a smooth background (solid blue curve). The solid data points show the yields associated with sequential proton decay through the 0^+_1 (red circle) and 2^+_1 (blue square) intermediate states of ^{12}O obtained for a gate on the fitted ^{13}F peak. The width of this gate is indicated by the horizontal error bars. The open data points give the same components for bins on either side of the ^{13}F peak in order to interpolate the background contributions in the peak gate. An interpolation was obtained from Gaussian fits to these data, which are shown by the dotted curves. The fitted yields per gate width have been scaled to put these data points on the same vertical scale (counts per 0.25 MeV) as the histogram.

In order to constrain which ^{13}F level we have observed, it is useful to consider the mirror charge-exchange reaction using a ^{13}B beam to make the mirror nucleus ^{13}Be. The mirror reaction at a similar beam energy of $E/A = 70$ MeV on a ^{9}Be target was performed by Marks *et al.* [17] who argued that it should only populate positive-parity states. That work measured the $n + {}^{12}$Be invariant-mass spectrum, which was fit with a $J^\pi = 1/2^+$ ($E_T = 0.7$ MeV) and a $5/2^+$ ($E_T = 2.4$ MeV) state. A second fit was also considered adding another lower-energy $5/2^+$ state as suggested in the experimental work of Randisi *et al.* [18], though the existence of this state has since been criticized [19]. Thus, it seems reasonable that our observed peak is the mirror of either a $1/2^+$ or $5/2^+$ ^{13}Be state.

Based on ^{13}Be resonance energies, Fortune and Sherr have made predictions for the mirror ^{13}F states above the $p + {}^{12}$O threshold [20]. Adding the decay energy of ^{12}O$_{\text{g.s.}}$. obtained from the present dataset [12], the corresponding E_T values are shown by the arrows in Fig. 1. The two arrows for the $5/2^+$ prediction are based on two possible values for the energy of the mirror ^{13}Be state considered by Fortune and Sherr. These predictions clearly favor the assignment of the new state as $J^\pi = 5/2^+$.

Based on the results for the mirror reaction, we would expect the $1/2^+$ (assumed ground state) to be populated as well. Possibly this state is too wide to be the resolved from the background. We note some recent measurements of the

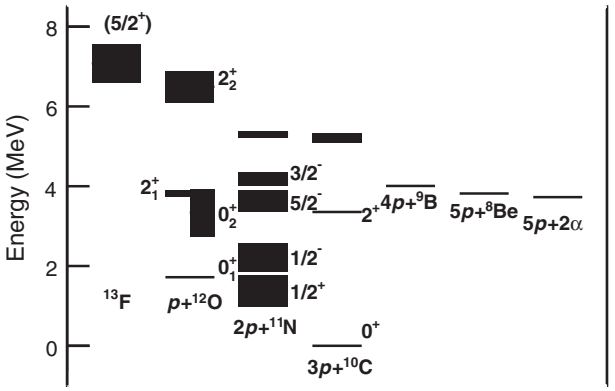

FIG. 2. Level diagram showing the location of the newly identified ^{13}F state relative to states in ^{12}O, ^{11}N, ^{10}C, ^{9}B, and ^{8}Be. Energies for the ^{12}O and ^{11}N excited states are from Ref. [12].

$1/2^+$-^{13}Be mirror state are $\Gamma = 1.70(15)$ [19] and 1.98 (34) MeV [17], and we would expect the more unbound mirror in ^{13}F to be wider than these. However, some other measurements of the $^{13}\mathrm{Be}_{1/2^+}$ state [18,21] give a much narrower width (0.75–0.8 MeV), making this argument less certain. Fortune and Sherr predicted a relatively narrow width of $\Gamma = 0.60(11)$ for the $1/2^+$ state in ^{13}F [20], which seems unlikely based on the range of widths for this mirror state.

Further information of the structure on the observed state can be gleaned from its decay mode(s). Figure 2 displays an energy-level diagram showing the 0^+_1, 0^+_2, 2^+_1, and 2^+_2 ^{12}O states that are energetically available following proton decay. All these ^{12}O states decay via democratic two-proton emission to the ^{10}C ground state with the higher 2^+_1 and 2^+_2 states showing some features of sequential decay through ^{11}N intermediate states [12]. There is also the possibility that the ^{13}F state undergoes a two-proton decay directly to a ^{11}N intermediate state or three-proton decays directly to ^{10}C. Of these possibilities, proton decay through the narrower 0^+_1 [$\Gamma = 51(19)$ keV] and 2^+_1 [$\Gamma = 155(15)$ keV] ^{12}O intermediate states can be most easily identified. For example, Fig. 3(a) shows the $2p + ^{10}$C invariant-mass distribution associated with a 1.15-MeV-wide gate in E_T around the peak maximum in the ^{13}F spectrum. For each $3p + ^{10}$C event, the invariant masses associated with the three possible $2p + ^{10}$C subevents were used to increment this distribution. As at most only one of these subevents could represent the decay of a real ^{12}O state, this spectrum has considerable extra background from the other subevents. However, above the background, one can resolve peaks associated with the 0^+_1 and 2^+_1 states whose centroid energies are indicated by arrows.

The measured ^{12}O distribution has been fit with contributions from sequential proton decays through the 0^+_1, 2^+_1, and 2^+_2 states deployed within our Monte Carlo

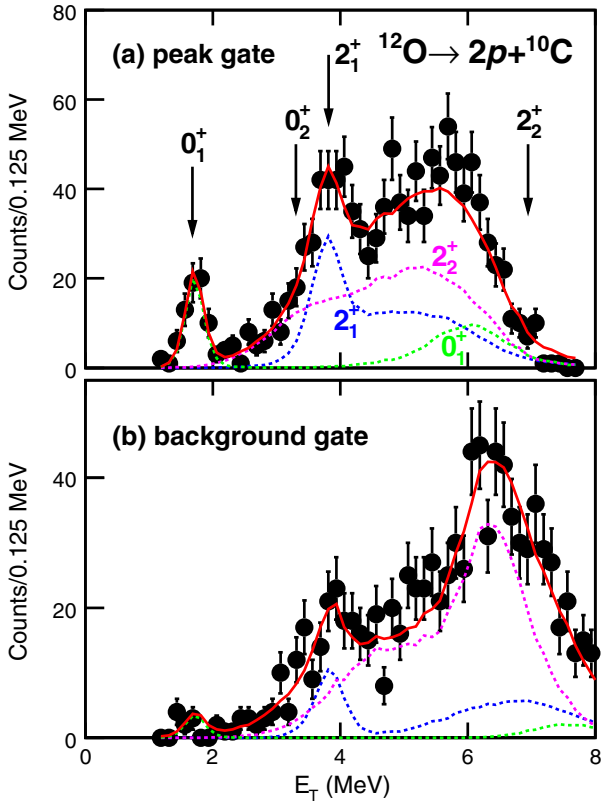

FIG. 3. Spectra of decay energy for ^{12}O determined from the invariant mass of the three possible $2p + ^{10}$C subevents from each detected $3p + ^{10}$C events. (a) Events that lie in a 1.15-MeV-wide gate centered on the ^{13}F peak, while (b) is for events in a background gate $8 < E_T < 9.3$ MeV. The red solid curve is a fit to this spectrum with contributions (dotted curves) from sequential proton decay through the 0^+_1 (green), 2^+_1 (blue), and 2^+_2 (magenta) intermediate states of ^{12}O. The arrows show the centroid decay energies of the known ^{12}O states.

simulations. In these simulations, the E_T for ^{13}F is divided between the kinetic energy of the first-emitted proton and the E_T for the ^{12}O intermediate state based on a distribution constructed from the product of the penetration factor for proton emission times the measured line shape of the intermediate state. In the subsequent $2p$ decay of the ^{12}O states, the experimental momentum correlations between the decay products from Ref. [12] were sampled and the experimental resolution and selection bias was then included. The fitted distribution is shown as the solid red curve and the contributions from the three decay paths are shown as the dotted curves. As for the experimental histogram, E_T values from all three possible $2p + ^{10}$C subevents are included in the simulated distributions. We tried including a contribution from decay through the wide 0^+_2 ^{12}O state, but this is excluded by the fit. The simulated distribution for decay to $^{12}\mathrm{O}_{\mathrm{g.s.}}$ (green dotted curve) has two peaks, however, the higher-energy peak is not associated with a real state, rather it is from the subevents that include

the higher-energy proton directly emitted from ^{13}F and one of the lower-energy protons from the decay of ^{12}O. For the decay path through the wide 2_2^+ state (dotted magenta curve), the barrier penetration factors suppress decay through all but the low-energy tail of its line shape, so there is no peak at the centroid for this state. Compared to the other two contributions, the E_T distribution in this case is rather featureless and it is not clear that other decay processes, such as $2p$ decay to a wide ^{11}N state, would not give a similar distribution. However, the contributions through the 0_1^+ and 2_1^+ intermediate states are quite distinctive with the presence of narrow peaks and we can have confidence in the extraction of the magnitudes of these components.

The ^{12}O distribution in Fig. 3(a) corresponds not just to the events in the ^{13}F peak but also to the substantial background under it (Fig. 1). In order to perform a background subtraction, we have constructed and fit ^{12}O invariant-mass distributions for regions on either side of the ^{13}F peak in Fig. 1. Figure 3(b) shows the distribution and fit for an E_T region just higher in energy ($8 < E_T < 9.3$ MeV). In this case, the contribution associated with decay through the 0_1^+ intermediate state has dropped significantly, and a peak associated with decay through the 2_2^+ now becomes prominent. Overall fits to these neighboring regions were not as good as in Fig. 3(a), indicating the need for extra components. We therefore concentrated on fitting just the magnitude of the narrow peaks associated with decays through the 0_1^+ and 2_1^+ intermediate states. The results are shown as the open data points in Fig. 1, while the results for the peak gate are shown as the solid data points. The horizontal error bars give the width of the E_T gates used to construct and fit ^{12}O distributions. We find that these two components are restricted to E_T values below 10 MeV. This is at least partly a result of the detection efficiency as, for such decays, large E_T values imply that the first proton is ejected with a large kinetic energy, allowing it to be defected to angles outside of the HiRA acceptance.

To interpolate the background values for the peak gate, we have fitted the background points with a simple Gaussian dependence (dotted curves in Fig. 1). With these backgrounds, we find the ^{13}F peak has 21(12)% and 37 (19)% contributions associated with proton decays through the 0_1^+ and 2_1^+ ^{12}O intermediate states, respectively, with the remainder 42(23)% possibly associated with decays through the wider 2_2^+ state. Correcting for the simulated detection efficiencies of the three decay paths, these correspond to branching ratios of 40(16)%, 28(18)%, and 32(16)%, respectively. Note, the efficiency for decay to the ground state of ^{12}O is reduced compared to the other two cases due to the large kinetic energy of the first-emitted proton which, as mentioned previously, is poorly mated to the angular acceptance of HiRA.

As an alternative to the Gaussian interpolation we have also considered a linear interpolation between just the two background points on either side of the ^{13}F peak. In this case the relative contributions from decays through the 0_1^+ and 2_1^+ states stay the same, but now account for all the yield in the ^{13}F peak. This linear interpolation should be considered a limiting case for the 2_1^+ component as its background distribution in Fig. 1 is consistent with a maximum for an E_T value near the centroid of the peak. Thus, we conclude that decay branches through the 0_1^+ and 2_1^+ states are both substantial, possibly accounting for all decays, but a third significant branch, probably through the 2_2^+ ^{12}O state, is likely. With the uncertainty in the branching ratios, the partial decay width to $^{12}O_{g.s.}$ is 0.50(13) MeV. This can be compared to a single-particle estimate of 1.9 MeV in a potential model with Wood-Saxon nuclear, plus spin-orbit and Coulomb contributions ($r_0 = 1.17$, $a = 0.64$ fm, $r_C = 1.21$, $V_{so} = 6.4$ MeV) where the depth of the Wood-Saxon is adjusted to fit the experimental decay energy. In the standard ansatz, the ratio of these widths gives a spectroscopic factor of 0.26(7). This is small compared to the shell-model prediction of 0.67 using the WBP interaction in the *s-p-sd-fp* valence space for the mirror state [18], but consistent with Fortune and Sherr's value of ~0.22. However, Fortune and Sherr's predicted width of ~0.38(7) is too small as it does not include partial widths for decays to excited ^{12}O states.

The possibly of a significant decay branch through the 2_2^+ state is interesting, especially as the small barrier penetration factor should suppress this decay. This possibility would imply that the structure of this ^{13}F state has a substantial component where a proton is coupled to the 2_2^+ ^{12}O core, presumably in an $s_{1/2}$ single-particle orbit to maximize the penetration. The 2_2^+ ^{12}O core is predicted to have a mostly p-shell configuration [22]. Such a ^{13}F structure maybe be justified as this ^{13}F resonance is located just above the $p + {}^{12}O_{2_2^+}$ threshold (Fig. 2). In open quantum systems, coupling to the continuum can modify the single-particle structure and for near-threshold states leads to the formation of collective eigenstates, which couple strongly to the threshold channel and carry many of it characteristics [23]. These aligned states are a superposition of shell-model wave functions with the same quantum numbers. For charged particles, the collectivization is maximized for states located a little above the threshold energy. For example, in the unstable ^{16}Ne ground state, the predicted collectivization with the shell model embedded in the continuum was a maximum when its energy was 0.5 MeV above the $p + {}^{15}$F threshold, where the valence proton is in a $s_{1/2}$ level [23]. In our case, the ^{13}F centroid is 0.48(19) MeV above the $p + {}^{12}O_{2_2^+}$ threshold, right at the expected maximum of collectivization and thus suggests the observed state has aligned its structure to the $p + {}^{12}O_{2_2^+}$ configuration. However, there may be additional effects when considering the full three-body continuum.

In addition, we note that this state is also above the $4p + {}^{9}\mathrm{B}$, $5p + {}^{8}\mathrm{Be}$, and $5p + 2\alpha$ decay thresholds (Fig. 2), so higher-order continuum effects may also be important. No evidence for any decay branch of the observed state to the $5p + 2\alpha$ channel was found in the data, but the small experimental efficiency for detecting seven particles in coincidence means we have reduced sensitivity to this channel and to the $4p + {}^{9}\mathrm{B}$ and $5p + {}^{8}\mathrm{Be}$ channels that decay to it.

In conclusion, we have made the first observation of the isotope ^{13}F, which is located four neutrons beyond the proton drip line. The ^{13}F events were created in charge-exchange reactions with a fast ^{13}O beam colliding on a ^{9}Be target. The invariant-mass distribution of detected $3p + {}^{10}\mathrm{C}$ events displays a 1.01(27)-MeV-wide peak at a decay energy of 7.06(9) MeV sitting on a broad background. Based on predictions of Fortune and Sherr [20], this peak corresponds to the first $5/2^{+}$ excited state in ^{13}F. The ground state was expected to be populated, but was not resolved from the background.

The observed state is located 0.48(19) MeV above the threshold for proton decay to the second 2^{+} state in ^{12}O, suggesting that coupling to the continuum may lead to a strong rearrangement of the shell-model configurations aligning its structure to this exit channel. Although decay to this channel is suppressed by the small barrier penetration factor, there are some indications it does have a decay branch to this ^{12}O intermediate state. However, significant decay branches to the ground and first 2^{+} state of ^{12}O were observed.

This is a second invariant-mass study using charge-exchange reactions with a fast even-Z projectile on the proton drip line to make the first identification of a proton-rich isotope. The other case produced was ^{17}Na with a ^{17}Ne beam [7]. With a ^{20}Mg beam, one can consider making ^{20}Al.

This material is based upon work supported by the U.S. Department of Energy, Office of Science, Office of Nuclear Physics under Awards No. DE-FG02-87ER-40316, No. DE-FG02-04ER-41320, No. DE-SC0014552, and the National Science Foundation under Grant No. PHY-156556. J. M. was supported by a Department of Energy National Nuclear Security Administration Steward Science Graduate Fellowship under cooperative agreement No. DE-NA0002135.

*Present address: Lawrence Livermore National Laboratory, Livermore, CA 94550.

†Present address: Department of Nuclear Engineering, University of California, Berkeley, CA 94720.

[1] V. Goldberg, B. Roeder, G. Rogachev, G. Chubarian, E. Johnson, C. Fu, A. Alharbi, M. Avila, A. Banu, M. McCleskey, J. Mitchell, E. Simmons, G. Tabacaru, L. Trache, and R. Tribble, First observation of ^{14}F, Phys. Lett. B **692**, 307 (2010).

[2] W. A. Peters, T. Baumann, D. Bazin, B. A. Brown, R. R. C. Clement, N. Frank, P. Heckman, B. A. Luther, F. Nunes, J. Seitz, A. Stolz, M. Thoennessen, and E. Tryggestad, First two energy levels in ^{15}F, Phys. Rev. C **68**, 034607 (2003).

[3] V. Z. Goldberg, G. G. Chubarian, G. Tabacaru, L. Trache, R. E. Tribble, A. Aprahamian, G. V. Rogachev, B. B. Skorodumov, and X. D. Tang, Low-lying levels in ^{15}F and the shell model potential for drip-line nuclei, Phys. Rev. C **69**, 031302(R) (2004).

[4] F. Q. Guo, J. Powell, D. W. Lee, D. Leitner, M. A. McMahan, D. M. Moltz, J. P. O'Neil, K. Perajarvi, L. Phair, C. A. Ramsey, X. J. Xu, and J. Cerny, Reexamination of the energy levels of ^{15}F by $^{14}\mathrm{O} + {}^{1}\mathrm{H}$ elastic resonance scattering, Phys. Rev. C **72**, 034312 (2005).

[5] I. Stefan *et al.*, Probing nuclear forces beyond the drip-line using the mirror nuclei ^{16}N and ^{16}F, Phys. Rev. C **90**, 014307 (2014).

[6] F. de Grancey *et al.*, An above-barrier narrow resonance in ^{15}F, Phys. Lett. B **758**, 26 (2016).

[7] K. W. Brown, R. J. Charity, J. M. Elson, W. Reviol, L. G. Sobotka, W. W. Buhro, Z. Chajecki, W. G. Lynch, J. Manfredi, R. Shane, R. H. Showalter, M. B. Tsang, D. Weisshaar, J. R. Winkelbauer, S. Bedoor, and A. H. Wuosmaa, Proton-decaying states in light nuclei and the first observation of ^{17}Na, Phys. Rev. C **95**, 044326 (2017).

[8] D. Kostyleva *et al.*, Towards the Limits of Existence of Nuclear Structure: Observation and First Spectroscopy of the Isotope ^{31}K by Measuring Its Three-Proton Decay, Phys. Rev. Lett. **123**, 092502 (2019).

[9] D. Bazin, V. Andreev, A. Becerril, M. Doléans, P. Mantica, J. Ottarson, H. Schatz, J. Stoker, and J. Vincent, Radio frequency fragment separator at NSCL, Nucl. Instrum. Methods Phys. Res., Sect. A **606**, 314 (2009).

[10] M. Wallace, M. Famiano, M.-J. van Goethem, A. Rogers, W. Lynch, J. Clifford, F. Delaunay, J. Lee, S. Labostov, M. Mocko, L. Morris, A. Moroni, B. Nett, D. Oostdyk, R. Krishnasamy, M. Tsang, R. de Souza, S. Hudan, L. Sobotka, R. Charity, J. Elson, and G. Engel, The high resolution array (HiRA) for rare isotope beam experiments, Nucl. Instrum. Methods Phys. Res., Sect. A **583**, 302 (2007).

[11] T. B. Webb *et al.*, First Observation of Unbound ^{11}O, the Mirror of the Halo Nucleus ^{11}Li, Phys. Rev. Lett. **122**, 122501 (2019).

[12] T. B. Webb *et al.*, Particle decays of levels in ^{11,12}N and ^{12}O investigated with the invariant-mass method, Phys. Rev. C **100**, 024306 (2019).

[13] T. B. Webb *et al.*, Invariant-mass spectrum of ^{11}O, Phys. Rev. C **101**, 044317 (2020).

[14] R. J. Charity, K. W. Brown, J. Elson, W. Reviol, L. G. Sobotka, W. W. Buhro, Z. Chajecki, W. G. Lynch, J. Manfredi, R. Shane, R. H. Showalter, M. B. Tsang, D. Weisshaar, J. Winkelbauer, S. Bedoor, D. G. McNeel, and A. H. Wuosmaa, Invariant-mass spectroscopy of ^{18}Ne, ^{16}O, and ^{10}C excited states formed in neutron-transfer reactions, Phys. Rev. C **99**, 044304 (2019).

[15] R. J. Charity, K. W. Brown, J. Okołowicz, M. Płoszajczak, J. M. Elson, W. Reviol, L. G. Sobotka, W. W. Buhro, Z. Chajecki, W. G. Lynch, J. Manfredi, R. Shane,

R. H. Showalter, M. B. Tsang, D. Weisshaar, J. R. Winkelbauer, S. Bedoor, and A. H. Wuosmaa, Invariant-mass spectroscopy of ^{14}O excited states, Phys. Rev. C **100**, 064305 (2019).

[16] R. J. Charity, L. G. Sobotka, and J. A. Tostevin, Single-nucleon knockout cross sections for reactions producing resonance states at or beyond the drip line, Phys. Rev. C **102**, 044614 (2020).

[17] B. R. Marks, P. A. DeYoung, J. K. Smith, T. Baumann, J. Brown, N. Frank, J. Hinnefeld, M. Hoffman, M. D. Jones, Z. Kohley, A. N. Kuchera, B. Luther, A. Spyrou, S. Stephenson, C. Sullivan, M. Thoennessen, N. Viscariello, and S. J. Williams, Population of ^{13}Be in a nucleon exchange reaction, Phys. Rev. C **92**, 054320 (2015).

[18] G. Randisi *et al.*, Structure of ^{13}Be probed via secondary-beam reactions, Phys. Rev. C **89**, 034320 (2014).

[19] G. Ribeiro *et al.*, (R^{3}B Collaboration), Structure of ^{13}Be studied in proton knockout from ^{14}B, Phys. Rev. C **98**, 024603 (2018).

[20] H. T. Fortune and R. Sherr, Predictions for the first two positive-parity states of ^{13}F, Phys. Rev. C **86**, 034301 (2012).

[21] Y. Aksyutina *et al.*, Structure of the unbound nucleus ^{13}Be: One-neutron knockout reaction data from ^{14}Be analyzed in a holistic approach, Phys. Rev. C **87**, 064316 (2013).

[22] S. M. Wang, W. Nazarewicz, R. J. Charity, and L. G. Sobotka, Structure and decay of the extremely proton-rich nuclei ^{11,12}O, Phys. Rev. C **99**, 054302 (2019).

[23] J. Okołowicz, M. Płoszajczak, and W. Nazarewicz, On the origin of nuclear clustering, Prog. Theor. Phys. Suppl. **196**, 230 (2012).